AIIM

Association for Information and Image Management

1100 Wayne Avenue, Suite 1100
Silver Spring, Maryland 20910

301/587-8202

Centimeter

Inches

MANUFACTURED TO AIIM STANDARDS
BY APPLIED IMAGE, INC.

1 of 1

Progress Report
Experimental and Theoretical Investigation of High Gradient Acceleration

Submitted to
Department of Energy
Washington, D.C.

Prepared by
Dr. J. S. Wurtele
Dr. G. Bekefi
Dr. C. Chen
Dr. S.C. Chen
Dr. R.J. Temkin

Plasma Fusion Center
Massachusetts Institute of Technology
Cambridge, Massachusetts 02139

Duration of Research
Feb 1, 1992-Jan 31, 1993

January, 1993

DISCLAIMER

Contents

1 Summary

This report contains a technical progress summary of the research conducted under the auspices of DOE Grant No. DE-AC02-91-ER40648, " Experimental and Theoretical Investigations of High Gradient Acceleration". This grant supports three research tasks: Task A consists of the design, fabrication and testing of a 17GHz RF photocathode gun, which can produce 2ps electron pulses with up to 1nC of charge at 2MeV energy and at a 10Hz repetition rate. Task B supports the testing of high gradient acceleration at 33GHz structure, and Task C comprises theoretical investigations, both in support of the experimental tasks and on critical physics issues for the development of high energy linear colliders.

Research under Task A has made significant progress in completing the 17GHz photocathode RF gun system fabrication and testing. The system includes a 17GHz gun structure, an RF transport line from the 17GHz CARM to the cavity, a picosecond laser system, a timimg system linking the mode-locked laser and the CARM, and associated components such as vacuum equipment and diagnostics. Major advances includes the following: (i) Power absorption of over 90% in the prototype RF gun cavities has been achieved in cold tests. The coupling hole dimensions, locations, and shape were determined successfully using a theoretical model developed here and numerical simulation. The final working cavity has been tested. (ii) The RF transport line has been constructed and major components have been cold tested. The polarization converter converts the rotating polarization of the TE_{11} mode into fixed polarization with an efficiency of 98 %. The dual directional coupler shows a 60 dB attenuation in each direction as designed. The high power RF window presents a VSWR of 1.07 at 17.136 GHz. The Faraday cup to be used for current measurement is completely designed and is being fabricated. (iii) The construction of the picosecond IR laser system has been completed. Factory testing was successfully performed in December 1992. The laser system is currently under testing at MIT. (iv) The timing circuit components have been tested individually and will be integrated with the high power RF input line. (v) The first hot test of the RF gun with power from the CARM is scheduled for Spring, 1993.

The purpose of Task B is to demonstrate high gradient capability of accelerating structures driven by high power millimeter wave sources such as FELs, CARMs or gyrotrons. With this in view we are collaborating with the CLIC group at CERN where structures will be designed and constructed. The high power RF tests will be carried out at MIT.

A vigorous theoretical program has been pursued in critical problem areas related to advanced accelerator concepts, high gradient acceleration, and the basic equilibrium, stability, and radiation properties of intense charged particle beams. Broadly speaking, our

research continues to make significant contributions in the following areas: (i) Investigations of novel accelerator concepts using RF power, including two-beam accelerators and cyclotron resonance laser (CRL) accelerators, (ii) Investigation of critical physics issues in plasma accelerators, such as the laser-hose instability, (iii) Investigations of RF sources including the free-electron lasers, cyclotron resonance masers and novel two-stream amplifiers and (iv) Studies of coherent structures and particle dynamics in nonneutral plasmas and beams.

This report is organized as follows. The status of the RF photocathode gun is summarized in Sec. 2, the status of the high gradient 33GHz acceleration, using a 60MW free-electron laser, is summarized in Sec. 3, and theoretical research is summarized in Sec. 4. Supporting material is contained in Appendices 1-10.

2 Experimental Research on RF Photocathode Guns at 17 GHz

2.1 Overview

The overall system schematic of the 17 GHz RF Gun experiment is shown in Fig. 1. We have conducted an intensive study on waveguide coupling of RF gun cavities both theoretically and experimentally. The main results are described in the following sections (2.2.1 - 2.2.4). Detailed theories are contained in Appendices 1 and 2. The RF transport line has been constructed, the testing results of the major components (polarization convertor, high power window, directional coupler) are summarized in section 2.2.5. and Appendices 3 and 4. The Faraday cup to be used for current measurement is completely designed and is described in section constructed. Factory testing was performed in December 1992. The details of the system are described in 2.2.7 and Appendix 5. The laser system is currently being tested at MIT.

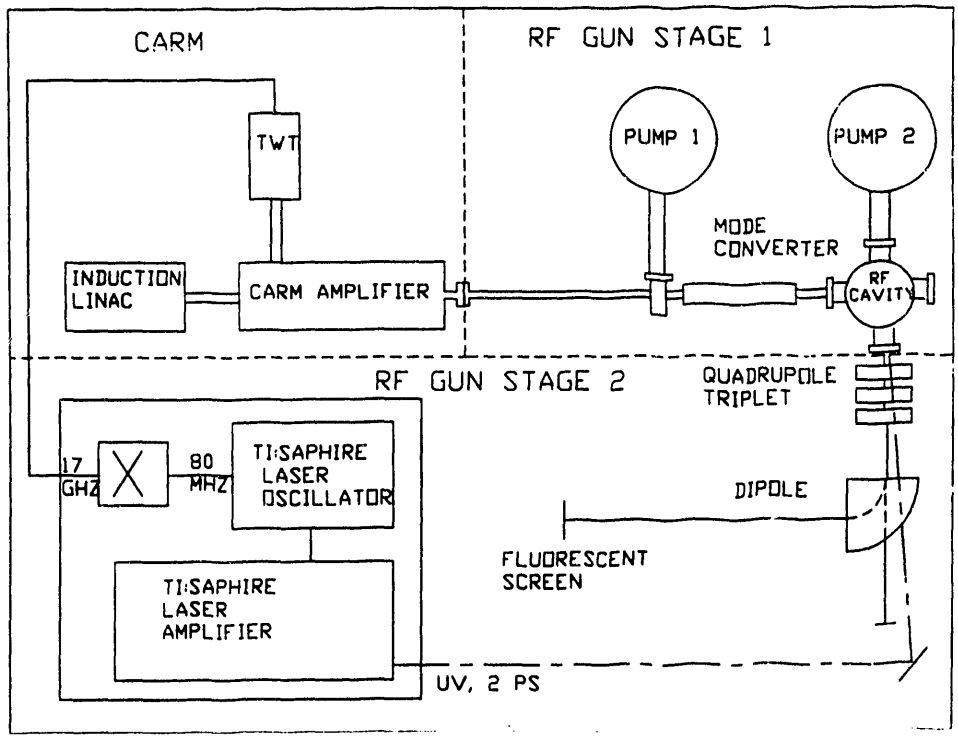

Figure 1: Schematic of the 17 GHz photocathode RF gun experiment.

2.2 Status of the Experimental Program

2.2.1 Cold testing of the RF gun cavities

The fractional reflected power (S11) from the waveguide-fed RF gun cavities was measured using a network analyzer. Fig. 2 shows the reflected power as a function of frequency. In this example, the two cavities have not been tuned. There are two clearly visible resonances, each of which corresponds to the absorption of most of the incident power in one cavity. The width and location of the resonances show that the two resonances are about 100 MHz apart and that each cavity has a Q value of about 1000. Each cavity absorbs over 80% of the incident power. Fig. 3 shows the fractional reflected power as a function of frequency for the two cells after tuning. In this case, the two resonances merged into a single dip corresponding to power absorption of over 90%.

Three prototype cavities were tested in a series of experiments, each with different fabrication and assembly techniques. The coupling hole dimensions and locations were determined successfully. The final working cavity is being tested.

2.2.2 Coupling Theory for the RF Gun Cavity with Waveguide Sidewall Coupling

The TE_{10} waveguide mode is coupled to the cavity through two rectangular apertures, one on each cell of the cavity, to excite the desired π mode resonance. The waveguide is shorted at a multiple of one-quarter guide wavelength away from the apertures to maximize the incident field strength on the apertures.

Theoretically, the cavity's two cells can be modeled as two lumped RLC circuits driven by a certain current/voltage that represents the aperture fields. The aperture fields not only excite resonances in the two cells but also excite fields in the waveguide. By imposing proper boundary conditions on the apertures one can solve the apertures' fields and come up with an equivalent circuit representation for this coupling problem. The detailed theoretical study is given in Appendix 1.

The theoretical results of the above analysis are in good agreement with experimental results.

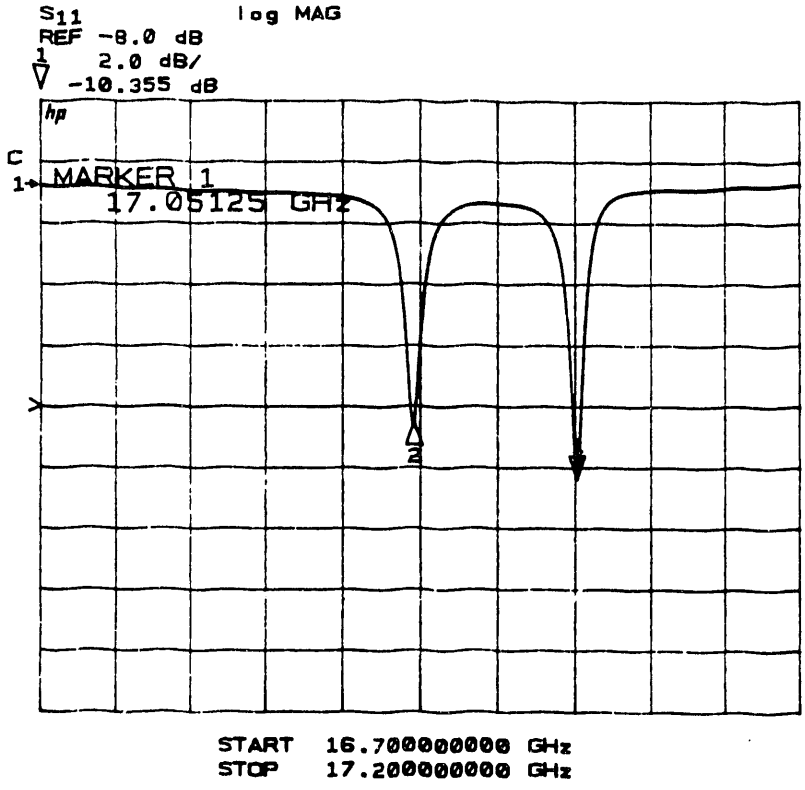

Figure 2: Reflected power spectrum of an untuned RF gun cavity

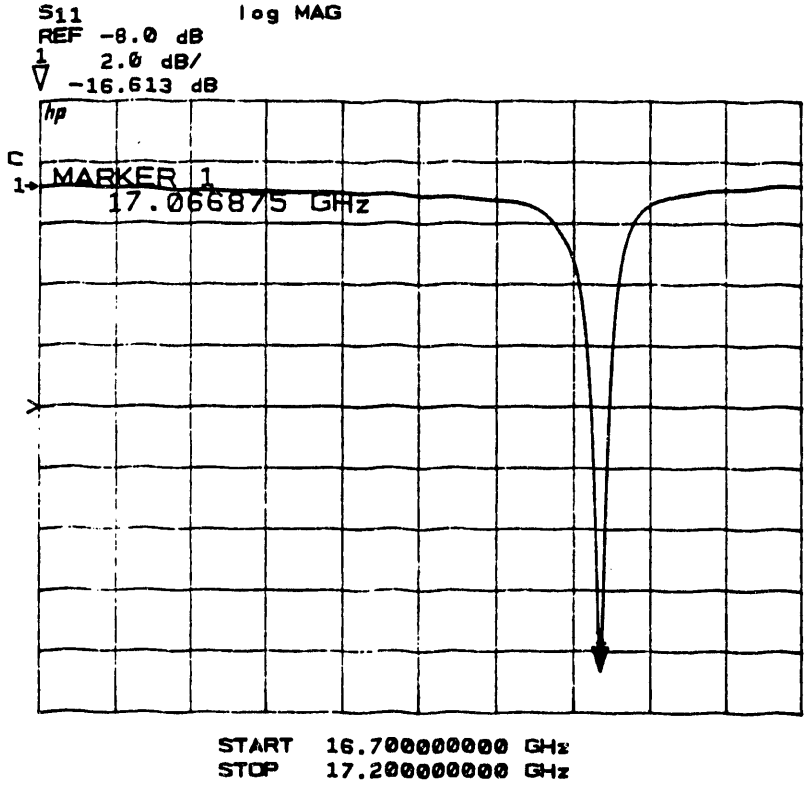

Figure 3: Reflected power spectrum of a tuned RF gun cavity

2.2.3 Coupling-Induced Frequency Effects in Sidewall-Coupled RF Gun Cavities

The tuning process exhibits many interesting coupling-induced effects specific to π-mode excitation. During the tuning process, the lower frequency cavity gradually develops a second characteristic frequency near the higher frequency cavity's. The closer the two cavities' frequencies are, the more pronounced the second absorption peak is. Note that this phenomenon is only present in the lower frequency cavity. The higher frequency cavity resonance, however, is not affected so dramatically by the coupling. The reason behind the observed asymmetry was studied theoretically.

Finally, when the two cavities are tuned up, the overall resonance occurs at a frequency higher than both of the original cavity frequencies. The frequency upshift is proportional to the coupling strength between the two cavities.

A coupled oscillator model was developed to explain the experimental observation. Details of the model can be found in Appendix agreement with experimental results.

2.2.4 Design and Testing of the RF Gun Vacuum Assembly

There has been a major design improvement in the vacuum design for the photocathode RF gun. In the previous scheme, the cavity and waveguide were in air and the gun cavity is pumped through holes in the waveguide sidewalls. In the new scheme, both the cavity and the waveguide are inside a vacuum chamber and the whole chamber is pumped. The new scheme provides the following advantages: First, the potential waveguide wall deformation due to the pressure difference inside and outside the waveguide is no longer a concern. Second, the monitor/tuner junction in the cavity walls need not be vacuum tight, thus simplifying the monitor/tuner design. Third, the cavity is pumped directly through the exit hole and the tuner/monitor holes, which we believe is more effective. Last but not least, it provides us with a great flexibility for the future addition of diagnostics through the use of other vacuum ports. The vacuum chamber, which is a modified five-way cross, is shown in Fig. 4. It is connected to a RF transport line, a viewport, an ion pump, a beam line, and two tuner/monitor sets. The vacuum chamber has been tested and is pumped down to $10^{-8} Torr$ with a 150 l/sec turbo pump alone.

2.2.5 RF Transport Line Testing

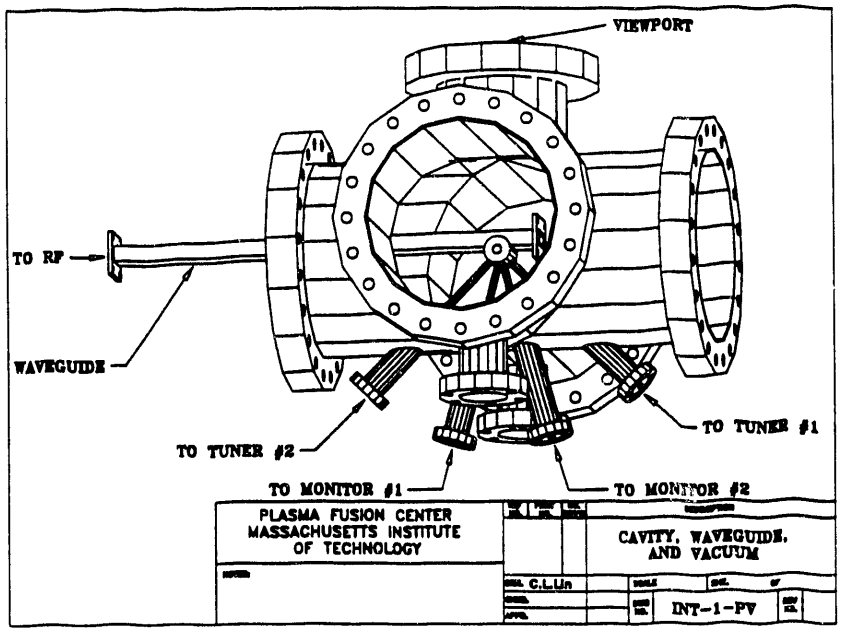

Figure 4: Vacuum chamber.

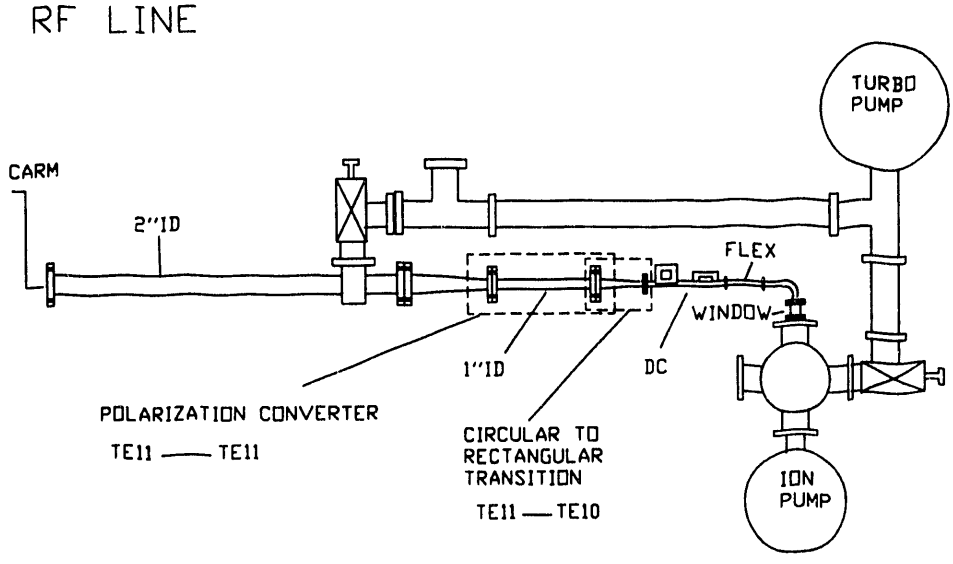

Figure 5: RF transport line.

The power source used to feed the RF cavity is a Cyclotron AutoResonance Maser (CARM) developed at MIT. The CARM will deliver 5MW peak in a pulse of 30 ns at a repetition rate of 10 Hz. The RF exits the CARM in a rotating polarization of the TE_{11} mode and must be converted to TE_{10} mode in the rectangular waveguide that couples to the RF cavity.

The RF transport line, whose schematic diagram is shown in Fig. 5, has been designed and constructed. A 2 " ID, 6 ' long circular waveguide is connected at one end to the output window of the CARM and at the other end to a tapered circular waveguide that changes the ID from 2 " to 1 ". The mode converter, described in detail in Appendix 3, follows the taper and is composed of two parts: first, a circular piece of waveguide whose cross section has been slightly deformed to be elliptical converts the rotating polarization of the TE_{11} mode to linear; the TE_{11} linearly polarized in the circular waveguide is then converted, through a circular to rectangular transition, to TE_{10} in the rectangular waveguide. Between this piece and the waveguide coupler, the construction is modular and involves a dual directional coupler, a vacuum window, and a flexible waveguide. The total length between the CARM and the cavity is more than 10 feet. This length provides transit time isolation between the RF gun cavity and the CARM amplifier.

All components of the RF line have been constructed and tested (see Appendix 4). The forward and reverse coupling of the directional coupler have been measured to be 60 dB; the forward and reverse directivity are approximately 20 dB. The maximum VSWR for the flexible waveguide is 1.23. The VSWR for the high power RF window does not exceed 1.2 between 16.9 and 17.1 GHz. The efficiency of the mode converter is at least 98 %. All components have been vacuum leak checked.

2.2.6 Faraday Cup Design

The first diagnostic that will be used to measure the current (either dark current or photoemission current) is a Faraday cup. The time constants of the signals to be measured are very short (1-10 ps); therefore, the Faraday cup has to be very short or impedance matched in order to avoid reflections during the pulse leading to a loss of signal. The design adopted is a coaxial transmission line adapted to 50 Ohms. The mechanical drawing of the Faraday cup is shown on Fig. 6. It is composed of two parts: a copper rod, which collects the electrons and constitutes the central conductor of the transmission line, and a copper cylinder (Faraday cup housing) which is the outer conductor of the transmission line. Both are mounted on a reducing flange closing the vacuum chamber where the RF cavity is located. The end of the collector that collects the electrons is located less than one inch from the exit of the RF cavity, and the other end is connected to a type N connector whose

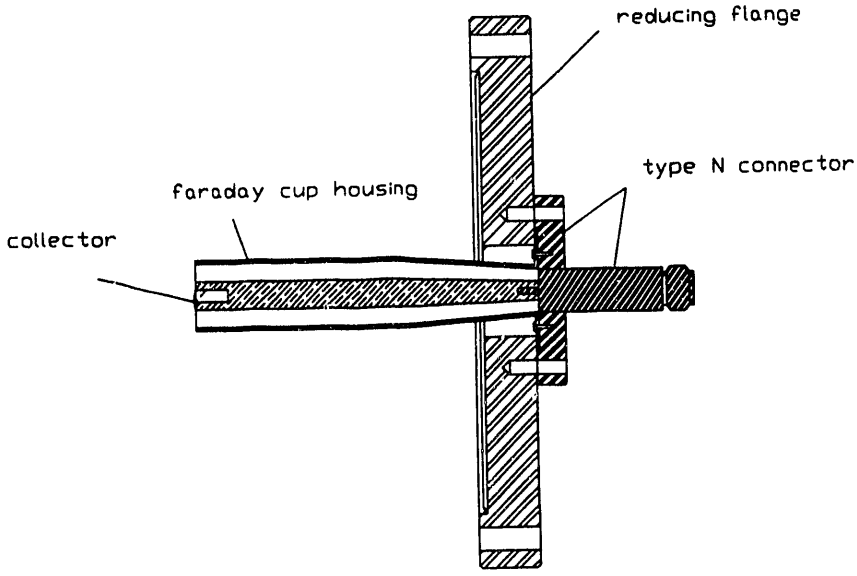

Figure 6: Faraday cup.

impedance is well defined to be 50 Ohms. The design is based on two formulae which give the characteristic impedance of, respectively, a coaxial and a bi-conical transmission lines. The coaxial line impedance is given by:

$$Z_0 = (\frac{1}{2\pi})(\frac{\mu}{\epsilon})^{1/2} ln(\frac{D}{d})$$

where ϵ and μ are the dielectric constant and permeability of the medium between the conductors, and $\frac{D}{d}$ is the ratio of the outer to inner diameters of the concentric conductors. In the vacuum $\frac{D}{d} = 2.303$ gives $Z_0 = 50$ Ohms. The bi-conical line impedance is:

$$Z_0 = (\frac{1}{2\pi})(\frac{\mu}{\epsilon})^{1/2} ln\left(\frac{cot(\theta_1/2)}{cot(\theta_2/2)}\right)$$

where θ_1 and θ_2 are half-angles of the inner and outer cones. The length of the bi-conical line is 2.5" and θ_1 and θ_2 are respectively 1.66 and 3.82 degree. The length of the coaxial line is 4" leading to a total length for the Faraday cup of 6.5".

When the electron beam hits the collector, secondary emission can occur; if these secondary electrons escape, the resulting current measurement is altered. To prevent this phenomena, a hole was drilled in the central rod as shown on Fig. 6, so that the secondary emission occurs inside the collector. The electron beam which exits the RF cavity has a diameter of 1.2 mm and a divergence of 40 mrad in the worst case. Then, if the Faraday cup is placed 1" away, the electrons will hit the collector in a spot of at most 1.5 mm in diameter. The stopping range for the electrons in copper at an energy of 2.3 MeV is 1 mm. The diameter of the collector is 1 cm and a hole of .5 cm diameter and 1 ' long has been drilled in its center. In this configuration, it is very improbable that any secondary electron can escape.

The signal arriving on the type N connector is too fast to be processed by any conventional oscilloscope. Therefore, it is necessary to integrate it. Several integrating boxes with different RC time constants can be connected to the type N connector. The integrated signal is then transported through a double grounded cable to a scope or a digital meter. By making several measurement with different RC time constants, one can in principle measure the charge in each micro-bunch.

2.2.7 Laser System Testing

The laser which provides the illumination for the RF gun photocathode is described in Appendix 5. The laser consists of a Ti:Sapphire laser, a Ti:Sapphire amplifier, and pump lasers. The design parameters are explained in Appendix 5 section 1. The final system design was chosen in 1992. The laser has been built, factory tested, and delivered to MIT. Currently, MIT is proceeding with system integration and construction of all necessary safety interlocks and devices. In the beginning of February MIT will complete system alignment and start testing. Also, the harmonic generator used to convert the output of the laser to ultraviolet has been designed and components are being purchased. The harmonic generator design is given in Appendix 5 section 3. After the laser system and the RF gun have been tested independently, the two will be integrated for the final series of experiments. The timing aspects of the laser will become vital at that time. The timing design of the laser is explained in Appendix 5 section 2.

2.3 Summary

We have conducted an intensive study on waveguide coupling of RF gun cavities both theoretically and experimentally. Power absorption of over 90% in the prototype RF gun cavities has been achieved in the cold tests. The coupling hole dimensions, locations, and shape were determined successfully. The final working cavity is being tested. Theoret-

ically, the cavity's two cells can be modeled as two lumped RLC circuits driven by a certain current/voltage that represents the aperture fields. The aperture fields not only excite resonance in the two cells but also excite fields in the waveguide. The tuning process exhibits many interesting coupling-induced effects previously unobserved. A coupled oscillator model was developed to explain the experimental observation. The theoretical results of the above analyses are in good agreement with experimental results.

The RF transport line has been constructed. The major components have been tested. The polarization converter converts the rotating polarization of the TE_{11} mode into fixed polarization with an efficiency of 98 %. The dual directional coupler shows a 60 dB attenuation in each direction as designed. The high power RF window presents a VSWR of 1.07 at 17.136 GHz. The Faraday cup to be used for current measurement is completely designed.

The construction of the picosecond IR laser system has been completed. Factory testing was successfully performed in December 1992. The laser system is currently under testing at MIT. The timing circuit components have been tested individually and will be integrated with the high power RF input line in the future.

3 Summary of Experimental Research on 33GHz Acceleration

The purpose of this program is to demonstrate high gradient capability of accelerating structures driven by high power millimeter wave sources such as FEL's, CARMs or gyrotrons. With this in view we are collaborating with the CLIC group at CERN where structures will be designed and constructed. The high power RF tests will be carried out at MIT (see Appendix 6 which is a letter from Dr. Ian Wilson describing a proposed structure as a beginning of our collaboration).

3.1 FEL Driver

The RF driver is MIT's highly successful Reversed Field FEL which is capable of supplying 60 MW at a frequency of 33 GHz. Our earlier studies are described in Appendix 7 in which the magnetics was barely long enough to reach saturation. During the past year we have extended the system length. The new results are prescribed in Figs. 7a,b,c. Linear power growth is $\simeq$30 dB/m in the Reversed Field configuration. Here $\simeq$70 MW at saturation has been obtained.

During the past year we have also found a new phenomenon, a frequency upshift in our FEL. Frequency upshifting of an electromagnetic wave incident on a rapidly time varying plasma medium is of considerable recent interest. Such upshifting can occur as a result of a time-dependent dielectric coefficient caused by changes in plasma density, or as a result of a rapidly moving plasma-vacuum boundary. Hitherto, studies have been confined to cases in which the dielectric is essentially a passive medium; that is, the amplitude of the wave propagating through it is constant in time and space. In this paper we report what we believe are the first frequency shift measurements in an active, lasing medium, in which the wave amplitude exhibits exponential growth. Here, the time-varying dielectric medium is modeled as an interaction between the pulsed relativistic electron beam of the FEL, the magnetic wiggler, and the copropagating electromagnetic wave launched into the system. The theoretical and computational modeling by Shvets and Wurtele is described in Section 4 below.

The experimental setup is illustrated in Fig. 8. An Alfred 650 sweep oscillator is used as a local oscillator, generating $\sim$6 mW at 23.39 GHz. This signal is combined in a magic tee with the FEL signal (previously attenuated to the appropriate milliwatt level) and then sent to a crystal rectifier (HP R422A). The nonlinear response of this crystal gives rise to the beat wave of the two signals, with a frequency of 10 GHz. This beat wave is then

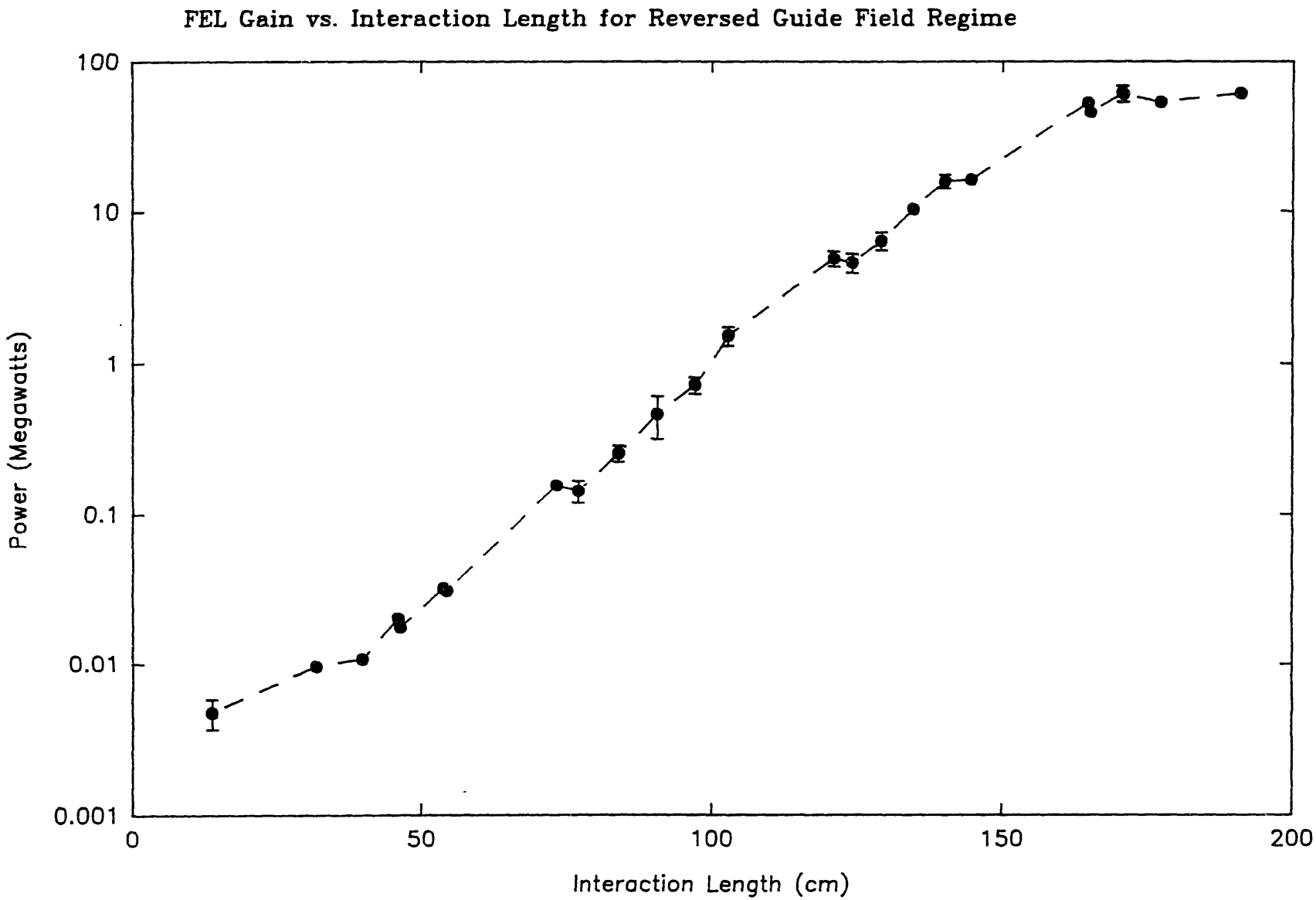
FEL Gain vs. Interaction Length for Reversed Guide Field Regime
Power (Megawatts)
100
10
1
0.1
0.01
0.001
0
50
100
150
200
Interaction Length (cm)

Figure 7a

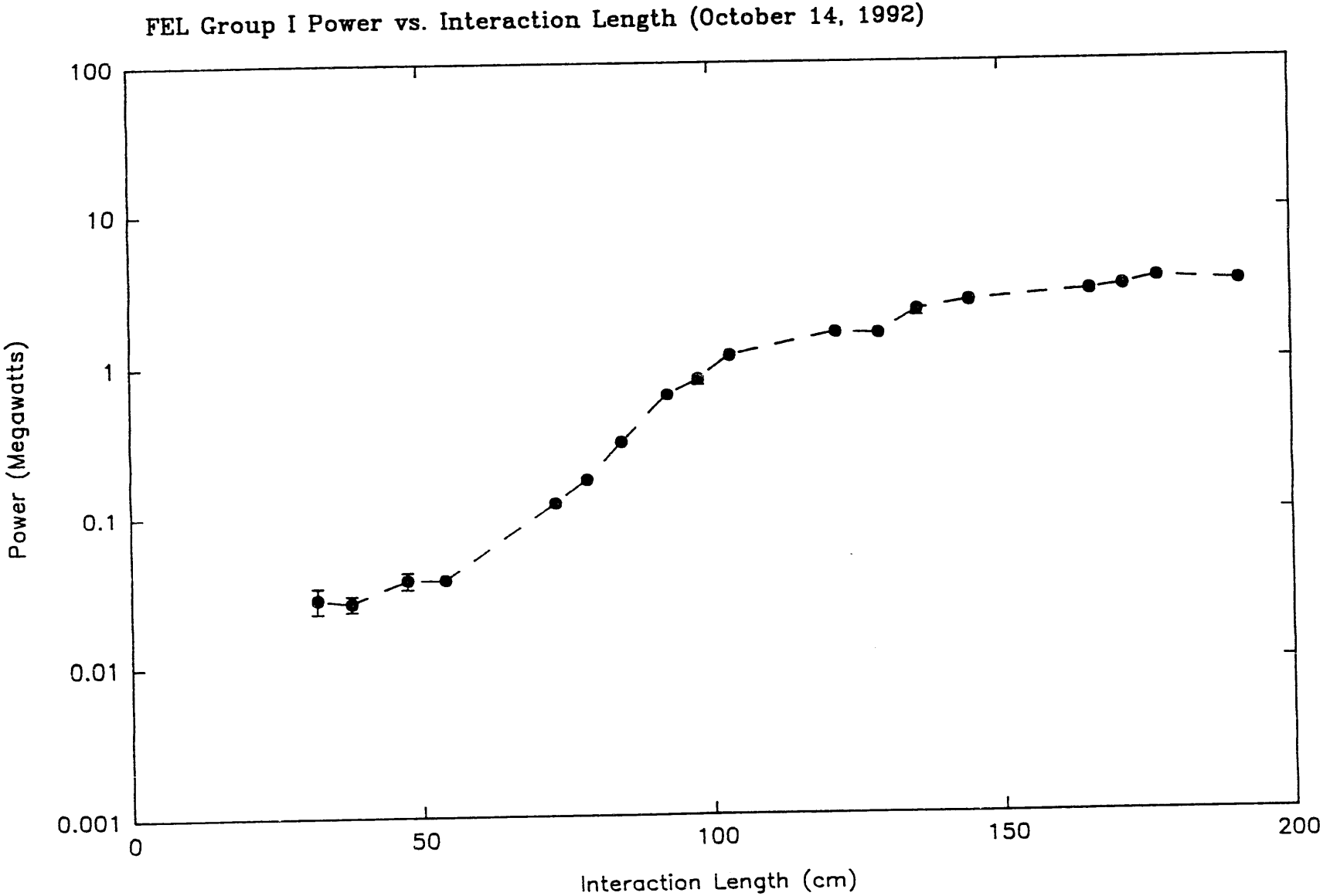
FEL Group I Power vs. Interaction Length (October 14, 1992)
Power (Megawatts)
100
10
1
0.1
0.01
0.001
0
50
100
150
200
Interaction Length (cm)

Figure 7b

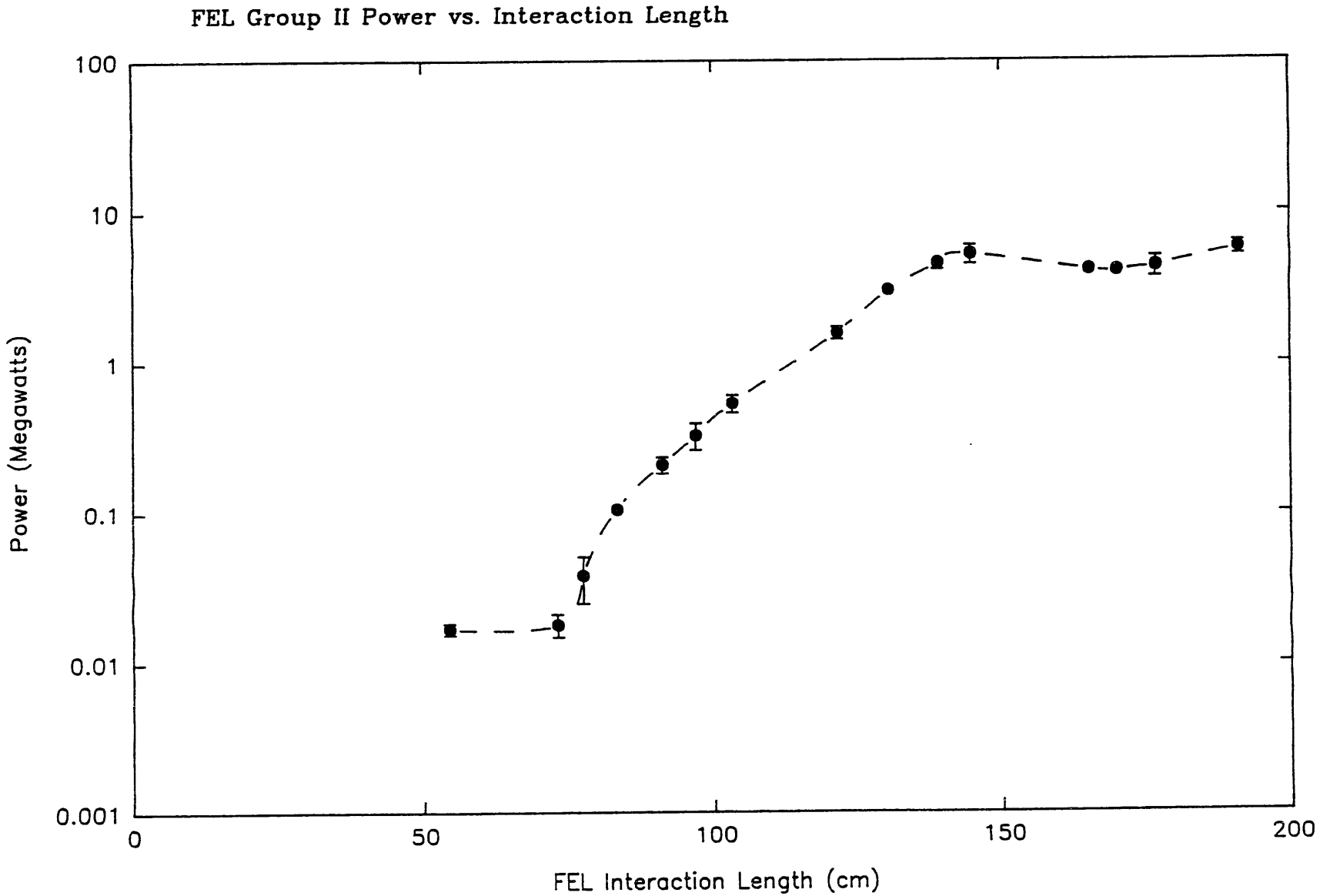
FEL Group II Power vs. Interaction Length
100
10
1
0.1
0.01
0.001
Power (Megawatts)
0
50
100
150
200
FEL Interaction Length (cm)

Figure 7c

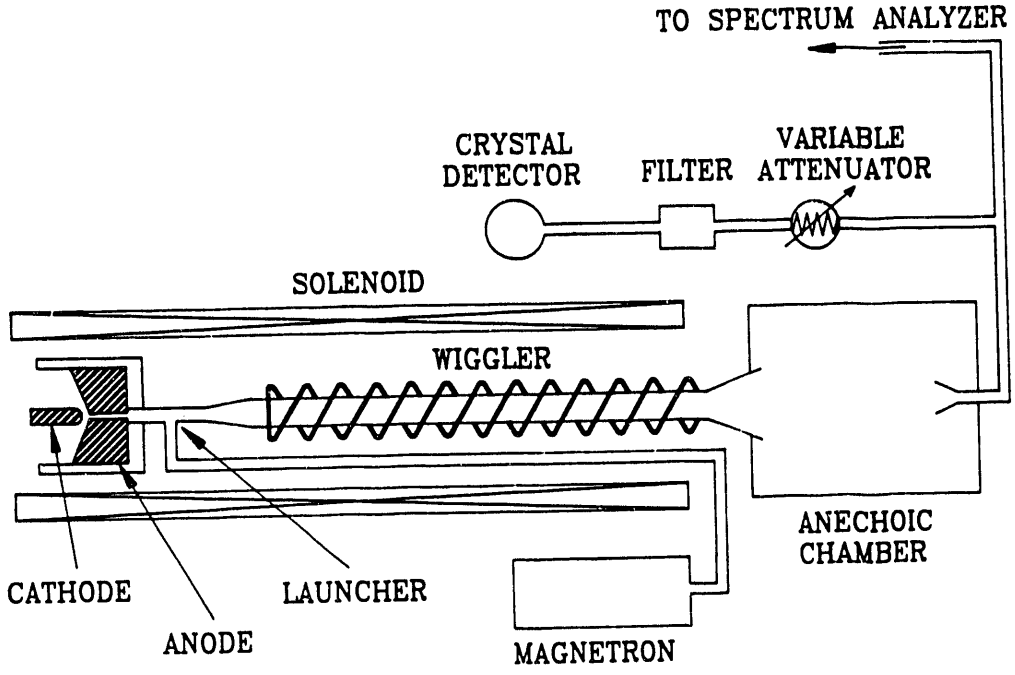
TO SPECTRUM ANALYZER
CRYSTAL DETECTOR
FILTER
VARIABLE ATTENUATOR
SOLENOID
WIGGLER
ANECHOIC CHAMBER
CATHODE
ANODE
LAUNCHER
MAGNETRON

(a)

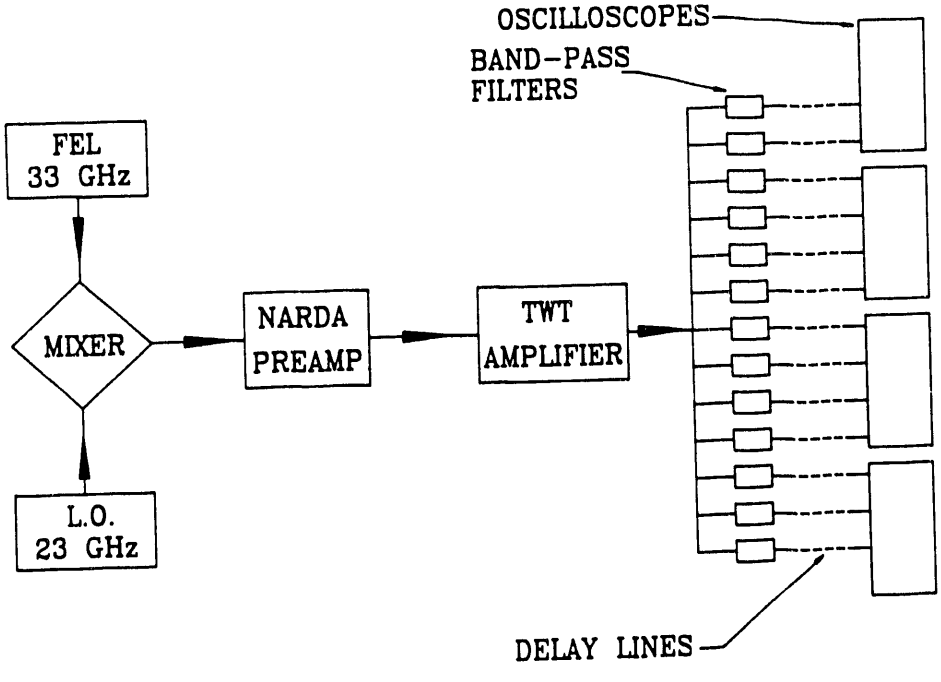
OSCILLOSCOPES
BAND-PASS FILTERS
FEL 33 GHz
MIXER
NARDA PREAMP
TWT AMPLIFIER
L.O. 23 GHz
DELAY LINES

(b)

Figure 8

amplified by a Narda 60164 solid state amplifier and by a Logimetrics TWT, and finally sent to the filter bank. The bank consists of 32 waveguide band-pass filters adjacent in frequency and each one 80 MHz wide. These channels are fed in parallel and each one has its own rectifier crystal (HP 33330B). Thus, the calibrated response of this array of rectifiers gives, on a single shot basis, the frequency spectrum of the output power. Figure 9 illustrates the measure upshift. Details of the experiment will be found in Appendix 8.

An understanding of the phase characteristics of the FEL are crucial in its application to driving high gradient accelerating structures. During the coming year we plan to conduct a series of phase measurements including phase stability.

3.2 Novel Concepts

We are also interested in exploring other novel concepts in high power radiation generation, and we have begun a study of the effect of slow wave structures on such systems as FELs, CARMs and gyrotrons. Figure 10 illustrates the system under present study. It consists of an array of metal posts with the electron beam propagating between them. We have observed a novel type of gyrotron interaction described in Appendix 9.

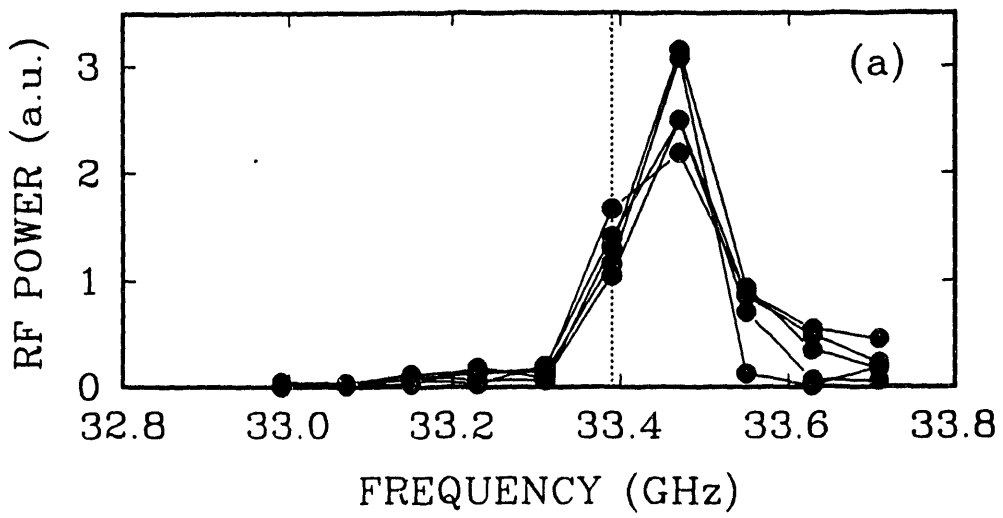

Figure 9

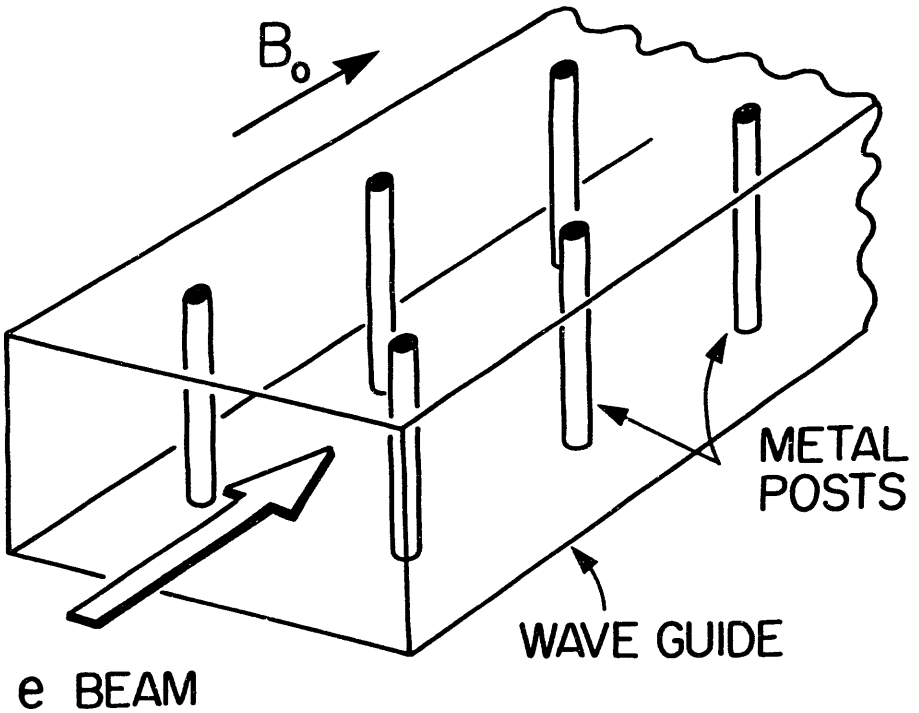

Figure 10a

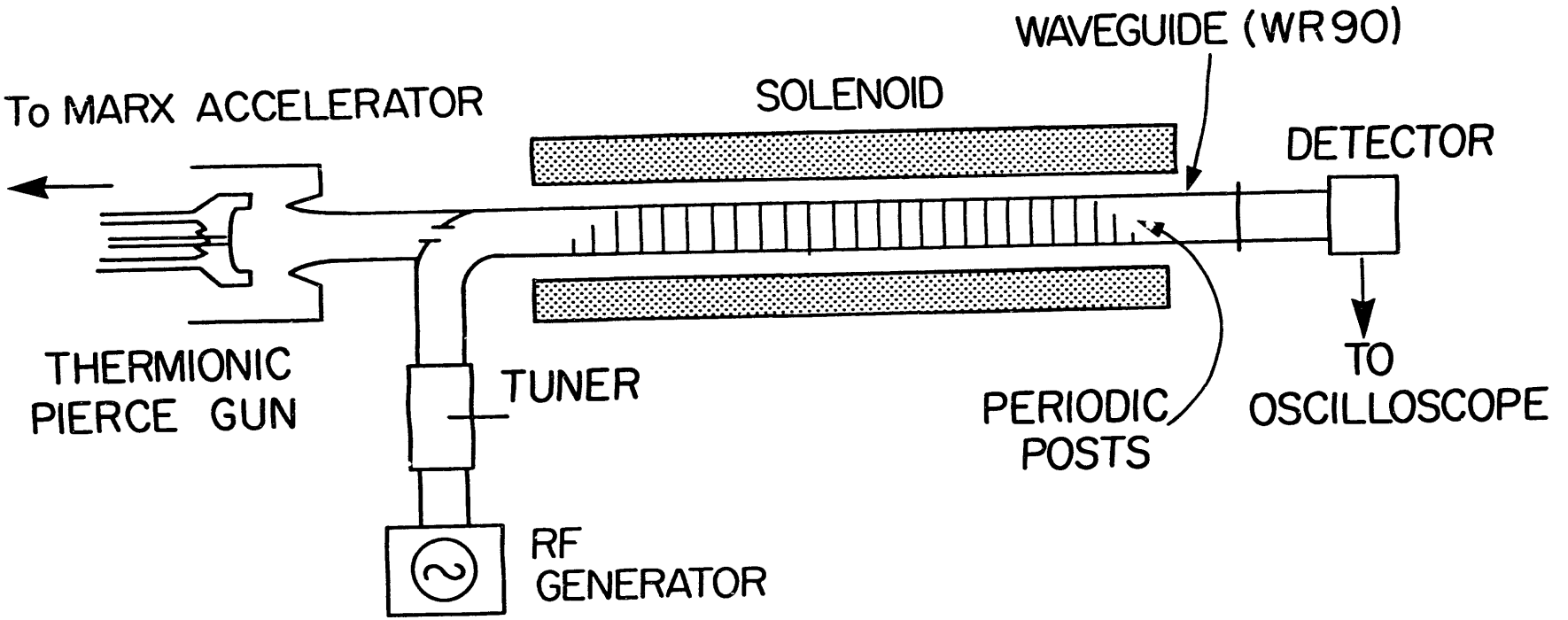
WAVEGUIDE (WR90)
To MARX ACCELERATOR
SOLENOID
DETECTOR
THERMIONIC
PIERCE GUN
TUNER
PERIODIC
POSTS
TO
OSCILLOSCOPE
RF
GENERATOR

Figure 10b

4 Summary of Theoretical Research Progress

This report summarizes technical progress and research accomplishments [1] on high gradient acceleration and advanced accelerator concepts, supported under Task C of Grant No. DE-AC02-92-ER40648, by the Department of Energy, during the period Feb. 1, 1992 through Jan 31, 1993. A vigorous theoretical program has been pursued in critical problem areas related to advanced accelerator concepts, high gradient acceleration, and the basic equilibrium, stability, and radiation properties of intense charged particle beams. Broadly speaking, our research continues to make significant contributions in the following three major areas in which the group has significant expertise:

1. Investigations of novel accelerator concepts using RF power, including two-beam accelerators [2]-[4] and cyclotron resonance laser (CRL) accelerators[5]-[7].
2. Investigation of critical physics issues in plasma accelerators [8], including the laser-hose instability [9] and the wakefield and guiding properties of hollow plasma channels [10]
3. Investigations of RF sources including the free-electron lasers [11]-[13], cyclotron resonance masers [14]- [16] and novel two-stream amplifiers[17],[18].
4. Studies of coherent structures and chaos in electron plasmas and beams ranging from a low-density, nonrelativistic, pure electron plasma column [19]-[21], and emittance growth in intense charged particle beams [22].
5. Studies of beam quality and RF coupling in photocathode guns. This theoretical work has been integrated into the description of the status of the experimental research in Task A.

The remainder of this report presents theoretical and computational advances in these areas.

4.1 Novel Accelerators Driven by RF

4.1.1 Two-Beam Accelerators

We are continuing our study of the two-beam accelerator with a comparative analysis [2],[3] of the relative performance of FEL-based and klystron based concepts. The work is based on an impedance model of standing wave radiation sources.

A formalism has been developed [4] for the analysis of collective instabilities in standing-wave systems. The analysis allows for the investigation of the coupled-cavity free-electron laser, relativistic klystrons and other high power microwave sources. Coupling from both the transverse and longitudinal motion of the beam is included in the calculation of the transverse and longitudinal impedances.

An understanding of high-power microwave sources and their scalings is crucial to the conception and design of high-energy electron-positron colliders. In fact, the tradeoffs between RF breakdown and beam break-up scalings is responsible for the current consensus that future linear colliders should be power by sources with an operating frequency in the 10-20 GHz range. For the lower frequencies, slow-wave devices have successfully produced, in proof-of-principle experiments, the power levels required. However, they have also exhibited what is, in fact, an intrinsic problem for such RF sources at short wavelengths: when the structure is small enough to couple effectively to the longitudinal beam motion, it also couples effectively to the transverse motion. This results in, among other undesirable phenomena, beam break-up and pulse shortening, as observed in recent relativistic klystron work at LLNL.

To circumvent this scaling, the coupling to the desired longitudinal mode should scale independently from that for those TM modes which produce beam break-up. One method of accomplishing this has been proposed in the form of a "standing-wave" free-electron laser (SWFEL). In this device, the drive beam couples to a TE mode through the oscillatory motion induced by a magnetic wiggler. Since the design orbit takes the beam off-axis, the premise of the Panofsky-Wenzel theorem fails, as does its conclusion, and strong coupling to a decelerating mode can be obtained with weak coupling to deflecting modes. In this work, we derive a formalism for quantifying such results, for the case of an idealized cavity, immersed in arbitrary plane polarized magnetic field. The formalism we derive, in essence, extends the wealth of work on longitudinal and transverse instabilities to include systems where the design particle orbit is curved within the cavity. In such "magnetized cavities" the coupling impedance describing longitudinal bunching can depend on the applied field. This permits one to enlarge the RF structure, so as to reduce undesirable transverse wakefields, while maintaining the desired longitudinal coupling.

Future work will compare the magnitudes of the new transverse impedances with the standard impedances from the holes between the cativies.

4.1.2 Cyclotron Resonance Laser Accelerators

There has been growing experimental interest recently in the cyclotron resonance laser (CRL) accelerator[6], an advanced accelerator concept of producing charged-particle beams at moderately or highly relativistic energies using an intense coherent electromagnetic wave and a guide magnetic field configuration. This novel accelerator has the following advantages over a conventional radio-frequency (RF) accelerator: (i) acceleration of a continuous beam without microbunches; (ii) use of an oscillator, not necessarily an amplifier, as driver; (iii) use of a smooth-wall structure to avoid breakdown problems; and (iv) a high duty factor of acceleration. It is compact in comparison with electrostatic accelerators which are bulky but capable of accelerating continuous charged-particle beams. In addition to these intriguing features, there is a variety of potential applications of CRL accelerators. These include the following: (i) small electron source for advanced accelerator experiments; (ii) production of high-average-power charged-particle beams for material and chemical research, such as beam welding and waste treatment; (iii) x-ray generation; and (iv) coherent millimeter wave generation, to mention a few examples.

Theoretical and computational investigations of prospects and limitations of this concept were conducted [6]. In particular, it was found that there exists a maximum energy threshold and a maximum acceleration distance. It was shown in a one-dimensional single-particle model that the maximum energy gain and the maximum acceleration distance obey certain scaling laws for optimized systems. The maximum energy gain is limited primarily by the degree of wave dispersion and is almost independent of the strength of the driving wave field. The validity of these scaling laws was confirmed in three-dimensional, self-consistent, multiparticle simulations in the microwave regime.

Based on our scaling calculations and presently available intense lasers and microwave sources, microwave CRL accelerators were identified as a practical concept in either pulse or continuous-wave (cw) operation, while optical CRL accelerators require stringent conditions and therefore are of only theoretical interest. In a recent workshop held at Port Jefferson, a small electron source which may be used in advanced accelerator experiments was proposed [7] based on the principle of cyclotron resonance laser acceleration.

Although our analyses have focused primarily on a traveling-wave configuration, the scaling laws are expected to be valid in a standing-wave configuration which may be required to achieve high acceleration gradient with moderate microwave power. Further research is proposed to examine standing-wave CRL accelerators.

4.2 Plasma Accelerators

A review of plasma-based accelerator and beam transport conferences has been made [8]. Research has focused on developing an improved physics understanding of the propagation of laser pulses in underdense inhomogeneous plasmas. The stable propagation of laser pulses in underdense plasmas is fundamental to the development of laser wake-field accelerators. The laser pulses must be focused to a small spot size in order to generate a large amplitude plasma wave, and, thereby, a high accelerating gradient. The laser will, in free space, be focused only over a diffraction length (Rayleigh range) $Z_r = \pi a^2/\lambda$, where λ is the laser wavelength and a the laser waist at the focus. A homogeneous plasma, which has a dielectric constant $\epsilon = 1 - \omega_p^2/\omega^2$, will only enhance the tendency of the light to diffract. To achieve net acceleration of, say, a few GeV, with present terawatt lasers, will require propagation lengths of order 10-20 Rayleigh ranges, and TeV accelerators hundreds of Rayleigh lengths.

Several schemes have been proposed to overcome diffraction. Relativistic guiding relies on the energy dependence of the plasma frequency, $\omega_p^2 = \omega_{p0}^2/\gamma$, where $\gamma = \sqrt{1 + \vec{p}\cdot\vec{p}/m^2c^2}$. The electron momentum p will be largest where the laser pulse is most intense, and therefore the plasma frequency will be lower there, and the pulse will generate a nonlinear index of refraction which is larger at the center of the pulse than at the pulse edges. For the accelerator application, long-pulse operation is unsatisfactory- pulses much longer than a plasma wavelength lead to small density wakes and, therefore, to low accelerating gradients. Relativistically guided laser pulses also suffer from Raman sidescatter instabilities.

For the short pulses (of order a plasma wavelength) required to generate a wakefield, however, relativistic guiding is substantially reduced [23]. This is due to the tendency of the ponderomotive force of the front of the laser pulse to push plasma electrons forward and generate a density increase which balances the relativistic mass increase. The plasma frequency then has no transverse variation and cannot optically guide the laser pulse.

An alternative scheme which has been investigated [23] envisions guiding the laser pulse in a plasma density channel. The channel has a higher density on the outside than on the inside, resulting in an index of refraction of the plasma which decreases from the channel axis (due to the increase in plasma density). A fixed plasma channel is analogous to an optical fiber, and its guiding properties can be similarly analyzed. The plasma channel can be used to guide short pulses, and has been studied using an axisymmetric model [23].

4.2.1 The Laser-Hose Instability

A new instability in laser-plasma interactions has been analyzed. The instability arises when a laser pulse propagates through a plasma channel and is initially not centered on the channel axis. The resulting non-axisymmetric component of the ponderomotive force generates a non-axisymmetric perturbation of the channel. The channel, perturbed by the head of the pulse, will, in turn cause the tail of the laser pulse to deflect further off axis. Thus, the plasma couples different longitudinal slices of the laser pulse. Consistent with causality, a given slice of the pulse is acted on only by those slices ahead of it. The underlying physics is straightforward : the off-centered laser produces a ponderomotive force with a dipole component; this causes the surrounding plasma electrons to try to follow the laser pulse. This results in the "beam-chasing" instability, which makes a small laser-channel misalignment grow exponentially and displace the pulse from its path. For a given initial misalignment, the instability imposes a limit on the laser pulse length and on the distance the pulse can propagate without significant deflection.

Explicit growth rates have been obtained in a wide range of parameter regimes. Future investigations will examine the the influence of the nonlinearities in the unperturbed equation, relativistic electron velocities, coupling to higher order modes, different density profiles, and different pulse shapes.

4.2.2 Laser Wakefields and Guiding in Hollow Plasma Channels

In addition to the analysis of the laser-hose instability described above, which assumed for a plasma with an inverted parabola transverse profile, we have examined the wakefields and guiding in a hollow plasma fiber. Good agreement has been found between our analytic theory and particle-in-cell simulations. This work is described in detail in the attached reprint.

4.3 Coherent Sources

4.3.1 Free-Electron Lasers

The physics and technology of free-electron lasers (FELs) are intimately related to the accelerator community because FELs are important applications of particle accelerators and have the potential to power high-gradient RF accelerators, such as in two-beam accel-

erators. Under the auspices of this grant, several important aspects of the FEL have been investigated, including:.

(a) development of a three-dimensional axisymmetric (TDA) code for free-electron laser simulation [11], and (b) numerical and theoretical investigations of gain and efficiency in a collective FEL [12]. (c) spectral properties of FELs with time varying current and energy profiles [13].

Development of the TDA code for FEL simulation The TDA simulation code [24],[25] has been developed and is widely used in the FEL community. Presently groups at MIT, CEBAF, LBL, UCLA, BNL and elsewhere are using the simulation to study the performance of various optical FEL systems. The TDA simulation solves the averaged FEL equations with fully three dimensional particle motion and the paraxial wave equation (with azimuthal symmetry assumed for the wave). Versions of TDA now include wiggler field errors and tapering schemes, multiple passes, and harmonics. Since the commencement of this grant, a fully three-dimensional version of TDA has been developed and distributed. [11]. The radiation and space-charge fields are no longer assumed to be axisymmetric. The code can now accurately predict the diffractive losses due to wiggler errors and corrector fields and includes focusing from ion channels and quadrupoles. At present work is continuing on the development of a user manual.

Investigations of free-electron laser operation with a reversed guide field A theoretical study of the nonlinear performance of a FEL amplifier operating, with a reversed guide field, in the collective (Raman) regime has been conducted [12]. The FEL generates [26] up to $\sim$ 60MW of RF power at a frequency of 33.3 GHz and an efficiency of $\sim$ 27 %. Power saturation, efficiency, and synchrotron oscillations are studied as a function of RF input power, electron beam energy, current, wiggler field amplitude, and axial distance with the helical wiggler. At present, the theoretical and simulation studies conducted at MIT and elsewhere have not successfully reproduced gain and saturation levels for both the reversed field and the group II orbits. Roughly, the reversed field behaves according to standard FEL theory, but the combined high growth rate and low saturated power is not consistent with linear theory or nonlinear simulations. (More precisely, simulations that reproduce the group II results do not reproduce the reverse field results). Results from particle-in-cell simulations have indicated that there can be competition between the upper and lower FEL modes (intersections of the beam and waveguide modes). We have developed a novel two frequency code which will be used to investigate mode competition in both FELs and CARMs.

Frequency Shifting Phenomena in FELs The frequency shifting of light by a moving dielectric front and bulk ionization of gases has been extensively investigated theoretically and experimentally by numerous researchers. These studies have been restricted to passive dielectric systems–those which induce phase shifts but have negligible gain. The dielectric coefficient of an electromagnetic wave in an underdense plasma, $\varepsilon = 1 - \frac{\omega_p^2}{\omega^2}$, being the typical example. Similar physics can be expected in an active medium such as the FEL. Since any frequency shift will become a phase shift if the FEL is used as power source for high gradient structures, the frequency shifts must be fully understood and the limits they place on shot-to-shot jitter defined.

Two distinct parameter regimes, a high power high gain microwave amplifier and a low gain infrared oscillator have been studied in detail. The theory is compared with recent experiments [27] which report frequency upshifting the FEL microwave amplifier funded under Task B of this proposal.

The wave equation for the vector potential of the transverse EM wave including the FEL and plasma coupling is

$$(\frac{1}{c^2}\frac{\partial^2}{\partial t^2} - \frac{\partial^2}{\partial z^2} + k_\perp^2)\vec{A} = \frac{4\pi}{c}(\vec{J}_{nr} + \vec{J}_{fel}), \tag{1}$$

where the source term has two distinct contributions- $\vec{J}_{nr}$, from the usual (nonresonant) cold beam response to the EM wave, which is present in the absence of the wiggler, and a second term from the resonant FEL interaction. The resonant current J_{fel} is produced by the ponderomotive force of the EM wave beating with the magnetic field of the wiggler. The beam is bunched in the ponderomotive wave, and the wiggling bunches produce the current which synchronously drives the EM wave. In the linear analysis (to which we restrict ourselves in this paper), this results in an exponentially growing instability. Since the parameters of the electron beam can be time-dependent, this can potentially lead to frequency-changing phenomena. The FEL is subject to frequency shifts when the driving terms $\vec{J}_{nr}$ and $\vec{J}_{fel}$ are time-dependent.

The dispersion relation obtained (see attached preprint) for parameter appropriate to the experiment of Task B, can be written, if the beam has a small density gradient,

$$\omega_p^2(s) = \omega_{p0}^2 + \Delta\omega_p^2(s) \tag{2}$$

as

$$(\Gamma + \Gamma_{\rm diel})(\Gamma - \Gamma_{\rm sp}) = -\Gamma_{max}^2, \tag{3}$$

where Γ_{max} is the maximum growth rate, Γ_{nr} comes from the nonresonant time dependent beam-loading , Γ_{sp} describes the time-dependent coupling to the slow space-charge wave.

Solving Eq [3] for the real part of the gain, we obtain:

$$Re(\Gamma) = \frac{\Gamma_{sp} - \Gamma_{diel}}{2} \tag{4}$$

Thus the frequency change after an interaction length z is given by

$$\delta\omega = \frac{1}{2} z \frac{\partial(\Gamma_{diel} - \Gamma_{sp})}{c\partial s}. \tag{5}$$

This equation shows that the frequency shift occurs because of two distinct mechanisms: the usual cold beam dielectric shift (from the beam density) and the coupling to the slow space-charge wave, which is due to the FEL interaction. The beam dielectric shift is physically equivalent to that of a cold plasma and is extensively described in the literature, the second effect has not, to our knowledge, yet been analyzed.

For the FEL of Task B, the parameters agree with the experimentally observed shift. Further investigations area underway to determine the effect of frequency shift on the performance of FEL power sources for high gradient structures.

4.3.2 Cyclotron Resonance Masers

Progress has been made in studies of mode competition in the cyclotron autoresonance maser (CARM). In particular, we have obtained a class of exact large-amplitude traveling-wave solutions [14] to the nonlinear Vlasov-Maxwell equations describing an electron beam in a finite axial magnetic field or a one-dimensional collisionless magnetized plasma. These solutions describe nonlinear (transverse) electromagnetic waves which are complementary to the nonlinear (longitudinal) electrostatic Bernstein-Green-Kruskal (BGK) modes. Our formalism can be applied to a variety of important problems concerning the interaction of an intense electromagnetic wave with a magnetized plasma or a relativistic electron beam propagating in a uniform magnetic field. The stability properties of the traveling-wave equilibria, which is related to mode competition in the CARM, are being analyzed analytically and numerically.

4.3.3 Novel Two-Stream Systems

The generation of intense coherent radiation based on the principle of the relativistic klystron amplifier (RKA) has been a subject of current experimental and theoretical research. High-power RKAs have applications in wide areas, including the development of high-gradient, radio-frequency (RF) accelerators.

We have proposed recently a *novel* two-stream relativistic klystron amplifier in which the interaction of the slow space-charge wave on a fast electron beam with the fast space-charge wave on a slow electron beam leads to an amplification of stimulated beam modulation. (The modulation comes about as a results of the beating of fast and slow space-charge waves.) In this two-stream RKA concept, the input and output cavities are connected with a smooth drift tube without intermediate passive cavities. The removal of the passive cavities prevents the amplifier from self-oscillation, a problem often arising from a traveling-wave tube (TWT) type of interactions in the RKA with multiple passive cavities. The possibility of RF breakdown at the passive cavities is eliminated. Thus, the two-stream RKA has an advantage over the conventional single-stream RKA, particularly in high-gain, high-power operation.

After a calculation of the limiting current, the amplification and saturation of the stimulated beam modulation were analyzed using a cold-fluid model and particle-in-cell simulation. Good agreement was found between theory and simulation in the linear regime. Fully modulated intense relativistic electron beams were obtained at saturation.

In the analysis of the two-stream RKA, the axial magnetic field was assumed to be large so that the transverse motion of the beam electrons is negligible. When the axial magnetic field is moderate, however, the transverse motion of the beam electrons can be sizable. Under certain conditions, space-charge cyclotron modes can be excited via an unstable two-stream interaction. This unstable interaction was proposed [28] as a novel mechanism for the generation of coherent radiation, which requires neither high beam voltage nor high magnetic field. We have develop a two-dimensional self-consistent theory[18] describing the two-stream cyclotron maser interaction.

The nonlinear coupling of electromagnetic and space-charge waves in high-frequency, high-power, relativistic RKA is being investigated for the single- and two- stream configurations.

4.4 Coherent Structures and Chaos in Electron Plasmas and Beams

It has been observed in various experiments and computer simulations that the ubiquitous appearance of coherent structures plays an important role in describing the dynamics of nonlinear systems governed by nonlinear partial differential equations. Coherent vortex structures, characterized by strong spatial and temporal correlations, occur in a variety of systems ranging from non-neutral plasmas with circulating electron flow. Future work in this area will include a substantial effort in understanding the physics of emittance growth, energy spread and pulse shape in high current photocathode guns.

4.4.1 Pure Electron Plasmas in Asymmetric Traps

Pure electron plasmas are routinely confined within cylindrically symmetric Penning traps. Such plasmas have potential applications as lenses and sources for high energy accelerators, as well as in unique high resolution electron-positron scattering experiments.

The equilibrium, stability, and dynamics of pure electron plasmas have been studied extensively. Traditionally, these plasmas are confined in Penning-like traps with cylindrical equipotential walls. Since these traps are azimuthally symmetric, the canonical angular momentum of the confined plasmas is conserved. This limits the radial expansion of the plasmas and has been thought to be responsible for the excellent confinement properties of these traps. However, the azimuthal symmetry can be broken by applying asymmetric electrostatic perturbations on the cylindrical trap wall.

We have conducted theoretical investigations [19]-[21] of the static and dynamic properties of plasmas confined in traps with applied electric field asymmetries are investigated. Simple analytical theories and numeric simulations are used to predict the shapes of the stable noncircular plasma equilibria observed in experiments. Experimental results [19] prove that these asymmetries degrade, but do not destroy, the trap confinement properties. Because angular momentum need not be conserved, a new outlook is required to understand these plasmas.

For an $\ell = 1$ diocotron mode in a cylindrically symmetric trap, the plasma rotates as solid column in a circular orbit. In contrast, plasmas in systems with electric field asymmetries are shown to have a analog to the $\ell = 1$ mode in which the shape of the plasma changes as it rotates in a noncircular orbit. These bulk plasma features are studied with a Hamiltonian model. It is seen [21] that, for a small plasma, the area enclosed by the orbit of the center of charge is an invariant when electric field perturbations are applied adiabatically. The breaking of the invariant has been studied as well.

4.4.2 Chaos in Intense Charged-Particle Beam Propagation through a Periodic Focusing Channel

The physics of intense charged-particle beam propagation in a periodic focusing channel is of vital importance in the advanced accelerator development and applications. Many applications of advanced accelerators, such as heavy-ion fusion and advanced radiation generation, require beams with high brightness, i.e., low emittance and high current. The goal of our current research is develop a fundamental understanding of emittance growth, limitations on beam brightness, and the transition from non-equilibrium to equilibrium for

space-charge-dominated beams.

In a recent study [22], we analyzed the transverse dynamics of intense charged-particle beams propagating through an applied magnetic field configuration consisting of periodic solenoidal and/or quadrupole focusing magnets. In multi-beamlet regimes, which have applications in heavy-ion fusion, it was shown in numerical simulations that the self fields associated with nonuniform charge density distribution result in chaotic particle orbits. The largest Liapunov exponent λ was found to be positive for every macroparticle. The characteristic distance for the multiple beams to merge into a single-beam equilibrium was estimated to be of order $1/\langle\lambda\rangle \cong 10\ S$, where S is the channel period. This estimated value, which is one order of magnitude larger than the previously predicted value (i.e., one fourth of the wavelength of a plasma oscillation), is in good agreement with the experiments by Reiser, *et al.* [29].

References

[1] Three-year research proposal entitled "Experimental and Theoretical Investigations of High Gradient Acceleration,"supported by the Department of Energy, Division of Nuclear and High Energy Physics.

[2] J.S. Wurtele, D. H. Whittum and A.M. Sessler, "Comparative Study of Klystron and FEL Two-Beam Accelerators," to be published in the Proceedings of the International COnference on High Energy Accelerators, Hamburg 1992.

[3] A.M. Sessler, D.H. Whittum, J.S. Wurtele, "A New Formalism for Standing Wave Radiation Sources," to be published in Advanced Accelerator Concepts, (J. S. Wurtele, Ed., AIP, New York) to be published 1993.

[4] X. T. Yu, J.S. Wurtele and D.H. Whittum, "Generalized Coupling Impedance Formalism for a Cummulative Instability", Sin preparation.

[5] C. Chen, "Scaling Laws for the Cyclotron Resonance Laser Accelerator," Phys. Fluids **B3**, in press (1991).

[6] C. Chen, "Theory of Electron Cyclotron Resonance Laser Accelerators," *Physical Review* **A46**, 6654 (1992), and references therein.

[7] C. Chen, to appear in the Proceedings of Advanced Accelerator Workshop, Port Jefferson, New York, 1992.

[8] "The Role of Plasma in Future Accelerators", J. S. Wurtele, **Invited Review Paper**, Physics Fluids B, in Press, 1993.

[9] G. Shvets and J.S. Wurtele, "The Laser-Hose Instability", submitted for publication.

[10] T. Katsouleas, P. C. Chiou, C. Decker, W.B. Mori, J. S. Wurtele, G. Shvets, J. J. Su, "Laser Wakefield Acceleration and Optical Guiding in a Hollow Plasma Channel", to be published in Advanced Accelerator Concepts, (J. S. Wurtele, Ed., AIP, New York) to be published 1993.

[11] "Three Dimensional FEL Simulations", P. Jha and J. S. Wurtele, Nuclear Instruments and Methods in Physics Research, in press 1993.

[12] "Theory and Simulation of a Reversed Field Free-Electron Laser", G. Zhang, G. Shvets, and J. S. Wurtele, Nuclear Instruments and Methods in Physics Research, in press 1993.

[13] G. Shvets and J. S. Wurtele, "Frequency SHifting in Free-Electron Lasers", manuscript in preparation.

[14] C. Chen, J.A. Davies, G. Zhang, J.S. Wurtele, "Large-Amplitude Traveling Electromagnetic Waves in Collisionless Magnetoplasmas," Phys. Rev. Lett. **69**, 73 (1992).

[15] C. Chen, B.G. Danly, G. Shvets, and J.S. Wurtele, "Effect of Longitudinal Space-Charge Waves of a Helical Relativistic Electron Beam on the Cyclotron Maser Instability," *IEEE Transaction on Plasma Science* **PS20**, 149 (1992).

[16] H.P. Freund and C. Chen, "Comparison of Gyro-Averaged and Non-Gyro-Averaged Nonlinear Analyses of Cyclotron Autoresonance Masers," *International Journal of Electronics* **72**, 1005 (1992).

[17] C. Chen, P. Catravas, and G. Bekefi, submitted to Appl. Phys. Lett. (1992).

[18] C. Chen, G. Bekefi, and W. Hu, manuscript in preparation (1993).

[19] "Asymmetric Stable Equilibria in Nonlinear Plasmas", J. Notte, A. J. Peurring, J. Fajans, R. Chu, and J. S. Wurtele, Phys. Rev. Lett. 69, 3065 (1992).

[20] "Pure Electron Plasmas in Asymmetric Traps", R. Chu, J. S. Wurtele, J. Notte, A. J. Peurring, and J. Fajans, **Invited Paper**, Physics Fluids B, in Press, 1993.

[21] "Experimental Breaking of a Mode Adiabatic Invariant", J. Notte, J. Fajans, R. Chu and J.S. Wurtele, submitted for publication.

[22] R.C. Davidson and C. Chen, APS Bull. **37**, 1584 (1992).

[23] P. Sprangle, E. Esarey, and A. Ting, *Phys. Rev. Lett.* **64**, 2011 (1990); P. Sprangle, E. Esarey, J. Krall, and G. Joyce, *Phys. Rev. Lett.* **69**, 2200 (1992).

[24] T.M. Tran and J.S. Wurtele, "TDA - A Three-Dimensional Axisymmetric Code for Free-Electron Laser (FEL) Simulation," Comp. Phys. Comm. **54**, 263 (1989).

[25] T.M. Tran and J.S. Wurtele, "Free-Electron Laser Simulation Techniques,"

[26] M. E. Conde and G. Bekefi, "Experimental Study of a 33.3 GHz Free-Electron Laser Amplifier with a Reversed Axial Guide Magnetic Field,"

[27] M. Conde and G. Bekefi, submitted to PHYSICS OF FLUIDS

[28] G. Bekefi, J. Appl. Phys. **71**, 4128 (1992).

[29] M. Reiser, *et. al.* Phys. Rev. Lett. **61**, 2933 (1988).

PUBLICATIONS SUPPORTED ALL OR IN PART BY THIS GRANT

1. "High Gradient Acceleration in a 17 GHz Photocathode RF gun", S.C. Chen, C.L. Lin, B.G. Danly, R. J. Temkin, J. Gonichon, and S.T. Trotz, Proceedings of Beams 92 Conference, Washington DC in press 1993.

2. "The Role of Plasma in Future Accelerators", J. S. Wurtele, **Invited Review Paper**, Physics Fluids B, in Press, 1993.

3. "Experimental Breaking of a Mode Adiabatic Invariant", J. Notte, J. Fajans, R. Chu and J.S. Wurtele, submitted for publication.

4. "The Laser-Hose Instability", G. Shvets and J. S. Wurtele, submitted for publication.

5. "Three Dimensional FEL Simulations", P. Jha and J. S. Wurtele, Nuclear Instruments and Methods in Physics Research, in press 1993.

6. "Theory and Simulation of a Reversed Field Free-Electron Laser", G. Zhang, G. Shvets, and J. S. Wurtele, Nuclear Instruments and Methods in Physics Research, in press 1993.

7. "Laser Wakefield Acceleration and Optical Guiding in a Hollow Plasma Channel", T. Katsouleas, P. C. Chiou, C. Decker, W.B. Mori, J. S. Wurtele, G. Shvets, J. J. Su, to be published in Advanced Accelerator Concepts, (J. S. Wurtele, Ed., AIP, New York) to be published 1993.

8. "High Gradient Acceleration in a 17GHz RF Photocathode Gun", S. C. Chen, B. G. Danly, J. Gonichon, C. L. Lin, R. J. Temkin, S. Trotz and J. S. Wurtele, to be published in Advanced Accelerator Concepts, (J. S. Wurtele, Ed., AIP, New York) to be published 1993.

9. C. Chen, "Theory of Electron Cyclotron Resonance Laser Accelerators," *Physical Review* **A46**, 6654 (1992).

10. C. Chen, J.A. Davies, J.S. Wurtele, and G. Zhang, "Large-Amplitude Traveling Electromagnetic Waves in Collisionless Magnetoplasmas," *Physical Review Letters* **69**, 73 (1992).

11. C. Chen, B.G. Danly, G. Shvets, and J.S. Wurtele, "Effect of Longitudinal Space-Charge Waves of a Helical Relativistic Electron Beam on the Cyclotron Maser Instability," *IEEE Transaction on Plasma Science* **PS20**, 149 (1992).

12. H.P. Freund and C. Chen, "Comparison of Gyro-Averaged and Non-Gyro-Averaged Nonlinear Analyses of Cyclotron Autoresonance Masers," *International Journal of Electronics* **72**, 1005 (1992).

13. "Asymmetric Stable Equilibria in Nonlinear Plasmas", J. Notte, A. J. Peurring, J. Fajans, R. Chu, and J. S. Wurtele, Phys. Rev. Lett. 69, 3065 (1992).

14. "Pure Electron Plasmas in Asymmetric Traps", R. Chu, J. S. Wurtele, J. Notte, A. J. Peurring, and J. Fajans, **Invited Paper**, Physics Fluids B, in Press, 1993.

15. H.W. Chan, C. Chen, and R.C. Davidson, "Numerical Study of Relativistic Magnetrons," submitted for publication, *Journal of Applied Physics* (1992).

16. C. Chen, P. Catravas, and G. Bekefi, "Growth and Saturation of Stimulated Beam Modulation in a Two-Stream Relativistic Klystron Amplifier," to appear in *Applied Physics Letters* (1993).

17. "Amplification and Spontaneous Emission From a 33GHz Free-Elecron Laser with a Reversed Axial Guide Magnetic Field", M. Conde and G. Bekefi, IEEE Trans. Plasma Sci. 20, 240 (1992).

18. "Observation of Frequency Upshift in a Pulsed Free-Electron Amplifier", M. Conde, C. J. Taylor and G. Bekefi, submitted to Phys. Fluids 1992.

APPENDIX 4

Dual Directional Coupler

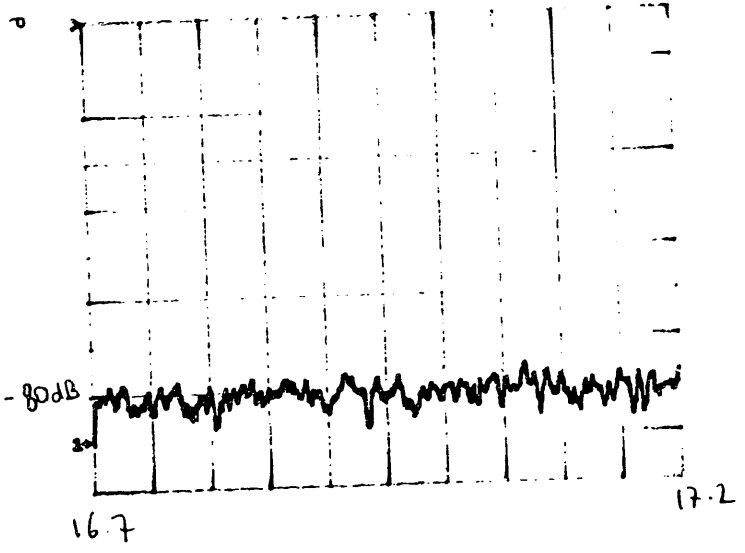

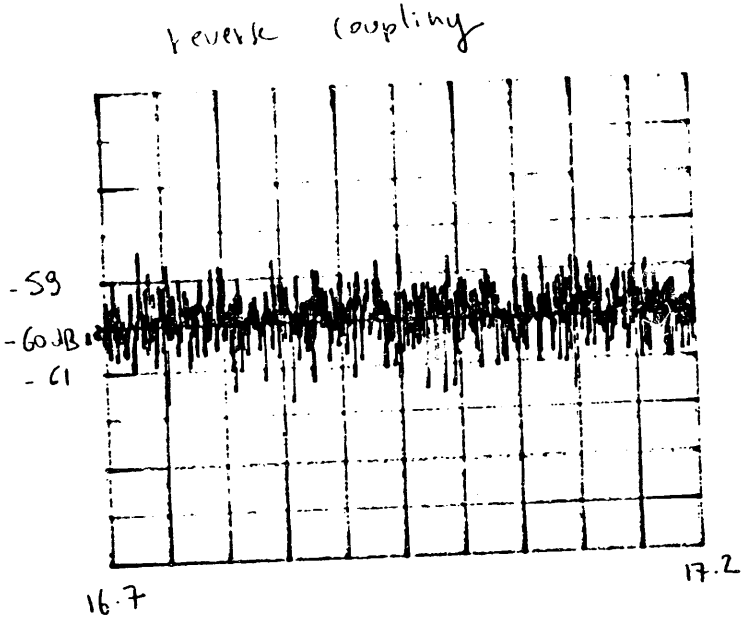

Dual Directional Coupler

Forward directivity

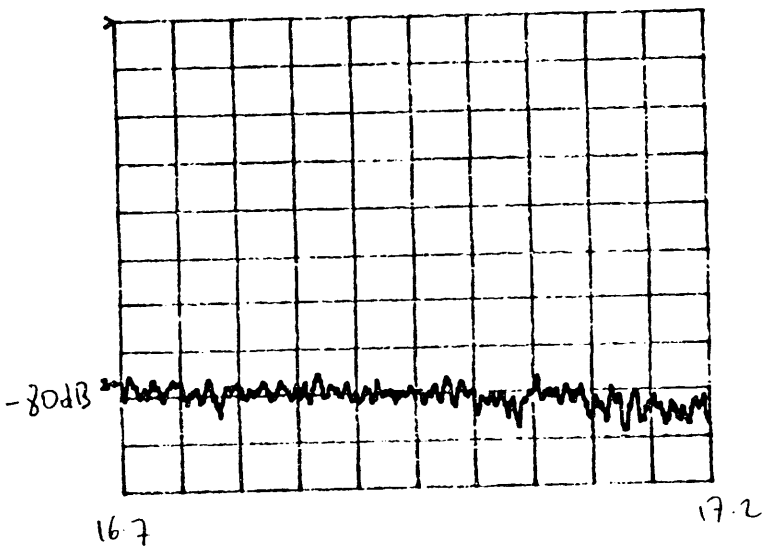

Reverse directivity

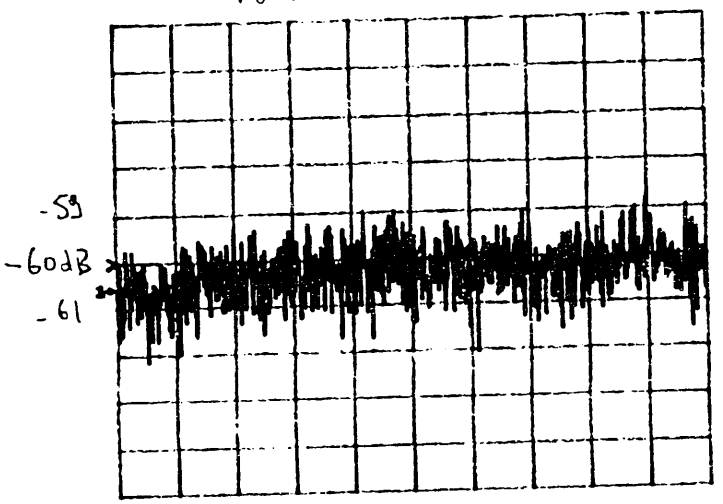

flex waveguide.

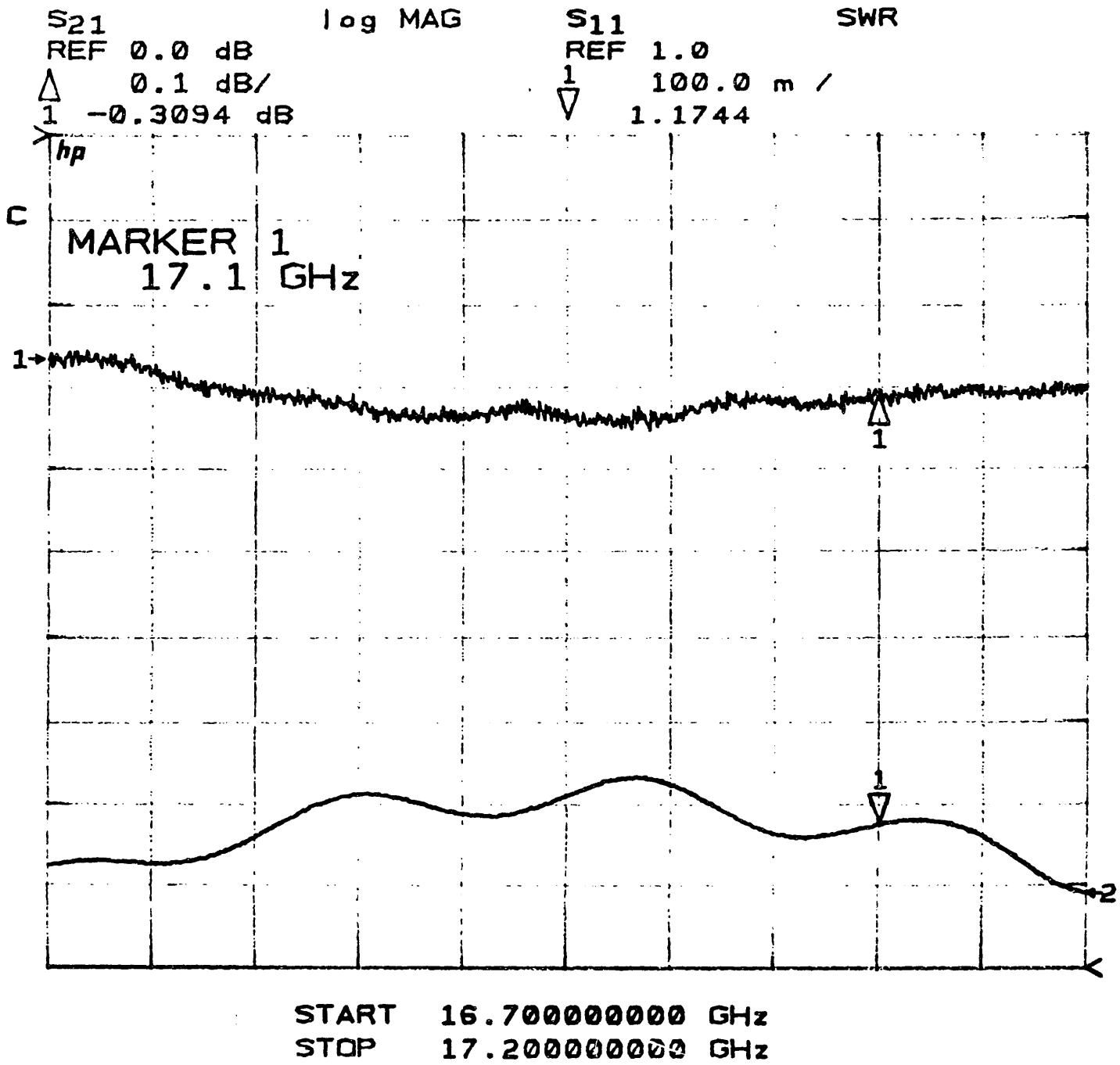

High power window

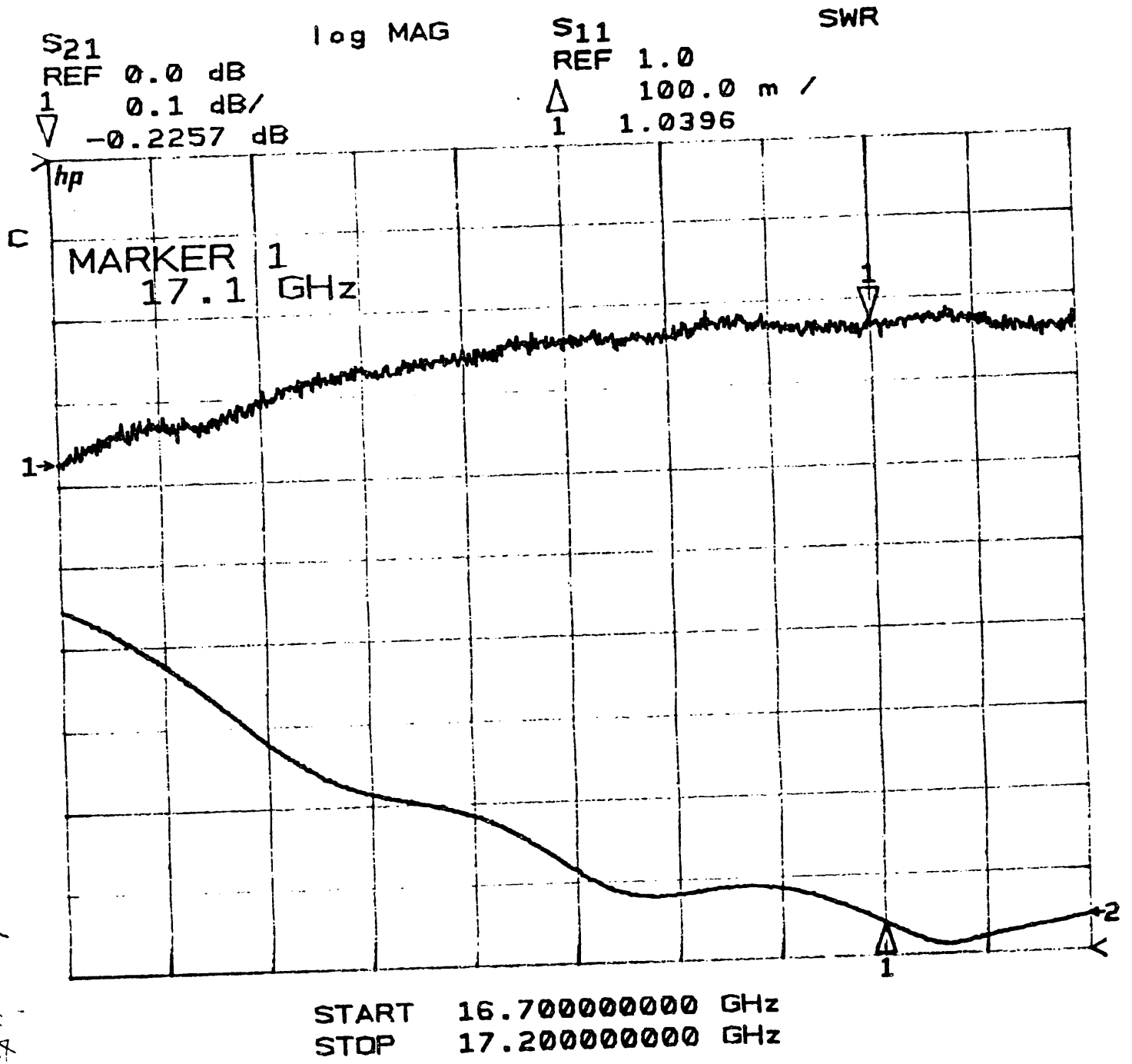

Prepared & reproduced, etc

DATE
FILMED
8/5/93
END